Targeted Cross-linking of the Human β-Globin Gene in Living Cells Mediated by a Triple Helix Forming Oligonucleotide†

Kazi Abdus Shahid, Alokes Majumdar,‡ Rowshon Alam,‡ Su-Ting Liu,‡ Jean Y. Kuan,# Xuifen Sui,‡ Bernard Cuenoud,§ Peter M. Glazer,# Paul S. Miller,|| and Michael M. Seidman*,‡

Laboratory of Molecular Gerontology, National Institute on Aging, National Institutes of Health, Baltimore, Maryland 21224, Novartis Pharmaceuticals Ltd, 4002 Basel, Switzerland, Department of Biochemistry and Molecular Biology, Bloomberg School of Public Health, Johns Hopkins University, Baltimore, Maryland 21205, and Departments of Therapeutic Radiology and Genetics, Yale University School of Medicine, P.O. Box 208040, New Haven, Connecticut 06520-8040

Received October 14, 2005; Revised Manuscript Received November 29, 2005

ABSTRACT: Triple helix forming oligonucleotides (TFOs) may have utility as gene targeting reagents for "in situ" gene therapy of genetic disorders. Triplex formation is challenged by negative charge repulsion between third strand and duplex phosphates, and destabilizing positive charge repulsion between adjacent protonated cytosines within pyrimidine motif third strands. Here we describe the synthesis of TFOs designed to target a site in the human β-globin gene, which is the locus for mutations that underlie the β-globinopathies, including sickle cell anemia. The target is an uninterrupted polypurine:polypyrimidine sequence, containing four adjacent cytosines, next to a psoralen cross-link site. Pyrimidine motif TFOs that contained four adjacent cytosines or 5-methylcytosines did not form stable triplexes at physiological pH, despite the introduction of otherwise stabilizing base and sugar analogues. We synthesized a series of pso-TFOs containing 2′-*O*-methyl (OMe) and 2′-*O*-aminoethoxy substitutions (AE), as well as 8-oxo-adenine (A^8) and 2′-*O*-methylpseudoisocytidine (P) as neutral cytosine replacements. Thermal stability measurements indicated that TFOs with A^8 did not meet criteria established in previous work. However, TFOs with P did form triplexes with appropriate T_m and k_{ON} values. A pso-TFO with AE and P residues was sufficiently active to permit the determination of targeting in living cells by direct measurement of cross-link formation at the target site. Our results validate the modification format described in our previous studies and indicate that P substitutions are an effective solution to the problem of targeting genomic sequences containing adjacent cytosines.

An efficient protocol for site specific genomic manipulation in living mammalian cells would have many research and practical applications. The strategy would require a gene targeting reagent that can find and bind a specific sequence with high affinity and specificity. Perturbation of the structural, or chemical, integrity of the target sequence would engage cellular functions that would eventually yield the desired change mutagenesis, gene conversion, gene knock in, etc. Such technology might eventually permit "in situ" gene therapy in which a disabling mutation in a critical gene would be restored to the wild type sequence in a clinically relevant cell population. This would avoid the complications associated with the random integration of an exogenous copy of a wild type gene under potentially disruptive control (*1*).

One approach to gene targeting is based on the DNA triple helix which can form when a third strand of nucleic acid lies in the major groove of an intact duplex (*2*). The most stable complexes are formed on polypurine:polypyrimidine elements, which are relatively abundant in mammalian genomes (*3*). The structure is sequence specific (*4*) and stabilized by two Hoogsteen hydrogen bonds between the bases in the third strand and the purine strand in the duplex. When the third strand consists of pyrimidines (pyrimidine motif), the triplets are T·A:T and C+·G:C. The third strand cytosine must be protonated at N^3 in order for a second Hoogsteen hydrogen bond to form.

Although triplex formation is relatively straightforward *in vitro*, in a cellular environment there are many impediments. Some are the result of the chromatin structure of mammalian genomes, which may preclude access to target sequences (*5*, *6*). We have shown that manipulations of the cell biology can (partially) overcome this restriction (*7*). We found that target access was greatest in S phase and very low in G_0. Similarly, transcriptional activation also renders targets more accessible to triple helix forming oligonucleotides (TFOs)[1] (*8*).

There are also many issues related to the chemistry and biochemistry of TFOs, particularly those in the pyrimidine

† The research described here was supported by the Intramural Research Program of the National Institute on Aging, National Institutes of Health.

* Corresponding author. Address: LMG/NIA/NIH, 5600 Nathan Shock Dr., Baltimore, MD 21224. Telephone: 410 558 8565. Fax: 410 558 8157. E-mail: seidmanm@grc.nia.nih.gov.

‡ National Institutes of Health.

§ Novartis Pharmaceuticals Ltd.

|| Johns Hopkins University.

Yale University School of Medicine.

[1] Abbreviations: TFO, triple helix forming oligonucleotide; Pso, psoralen; 5MeC, 5-methylcytosine; P, pseudoisocytidine; A^8, 8-oxo-adenine; AE, 2′-aminoethoxy.

10.1021/bi0520986 CCC: $33.50
Published on Web 01/24/2006

motif. Most of these have been addressed with some degree of success by introduction of base and sugar analogues into TFOs. Triplex formation by deoxyribose third strands imposes conformational restrictions on the TFO and some distortion of the underlying duplex. Typically triplexes formed by deoxyribose third strands are less stable than the underlying duplex. RNA analogue sugars can "preorganize" third strands, greatly reducing the entropic barriers to triplex formation and requiring relatively little distortion of the underlying duplex (*9*). Pyrimidine motif triplexes are generally unstable at physiological pH because of the requirement for cytosine protonation (cytosine pK_a = 4.5). This can be alleviated, at least in part, by the use of 5-methylcytosine (5MeC) (*10*). The stabilization by the methyl substitution results from stacking interactions and hydrophobic effects (*11*). This is effective for triplex sequences with isolated cytosines, and isolated cytosines make a considerable contribution to triplex stability. The positive charge partially reduces the negative charge repulsion between the third strand and the duplex (*12*), which is also ameliorated by magnesium ions (*13*). We have described pyrimidine motif TFOs containing 5MeC and 2′-*O*-methylribose that form triplexes at neutral pH that are as stable as the underlying duplex (*14*). On the other hand, targets with adjacent cytosines are more problematic. Triplex stability is greatly compromised by runs of cytosines, thought to be due to repulsion between the positive charges resulting from the N^3 protonation (*10*, *15*). Alternatively there may be a competition for protons by the adjacent cytosines (*16*). It has been shown that at physiological pH cytosine protonation is reduced in runs of cytosines relative to isolated cytosines (*11*). Several base analogues have been proposed as solutions to this problem. These are purine or pyrimidine analogues that are protonated at neutral pH such that two Hoogsteen hydrogen bonds with guanine are possible. They include 8-oxoadenine (*17*), 2′-*O*-methylpseudoisocytidine (*18*, *19*), and 2-amino-5-(2′-deoxy-β-D-ribofuranosyl)pyridine (2-aminopyridine) (*20*−*22*) (see also refs *23* and *24*). Although the results of biochemical analyses of TFOs with these derivatives are encouraging, their efficacy in biological assays has not been described.

Negative charge repulsion between the TFO and the duplex can be suppressed by the incorporation of 2′-aminoethoxy (AE) substitutions which are protonated at neutral pH (*25*, *26*). This modification stabilizes the C3′-endo conformation of the ribose and also forms a bridge with the $i - 1$ phosphate in the purine strand of the duplex (*26*). We have described the construction and characterization of TFOs containing a cluster of AE residues that are bioactive in a gene knock out assay in living mammalian cells (*7*, *27*, *28*). The TFOs were designed to target a sequence in the endogenous *HPRT* (hypoxanthine phosphoribosyl transferase) gene, which is commonly used as a mutation reporter gene. The target sequence was a 17 base polypurine:polypyrimidine element with isolated cytosines, terminating in an ideal site for cross-linking by psoralen. Psoralen linked TFOs containing different modifications were tested for activity in an assay that measured targeted mutagenesis of the *HPRT* gene (*14*, *27*, *28*). The *HPRT* mutation assay is straightforward and reports mutational events over a range of 5 orders of magnitude. However, most genes of interest for gene targeting do not lend themselves to simple selection based assays that report the desired event. Consequently, the TFO must be sufficiently active to allow detection of target binding with relatively insensitive biochemical methods. In this report we describe the development of a biologically active psoralen linked TFO designed to target a site containing adjacent cytosines in the human β-globin gene. The site is of interest because of the challenge to triplex formation presented by its sequence, and the many β-globinopathies in the human population resulting from mutations in the gene.

MATERIALS AND METHODS

Reagents. Reagent grade chemicals were used unless otherwise noted. HPLC grade acetonitrile was dried over calcium hydride. Anhydrous pyridine, dimethyl formamide, benzene, tetrahydrofuran, and methylene chloride were from Aldrich Chemical Co. Inc. 5-β-D-Ribofuranosyluracil (pseudouridine) was the generous gift of Dr. Kris Pankiewicz. The 5′-*O*-(4,4′-dimethoxytrityl)-5-methyluridine-2′-*O*-methyl-3′-*O*-(β-cyanoethyl-*N*,*N*-diisopropyl) phosphoramidite and the 5′-*O*-(4,4′-dimethoxytrityl)-5-methyluridine-2′-*O*-methyl-3′-*O*-succinamido-N^6-hexanamido N^3-propyl-controlled pore glass support were purchased from Chemgenes, Ashland, MA. Protected deoxyribonucleoside phosphoramidites, the N^4-acetyl-5′-*O*-(4,4′-dimethoxytrityl)-5-methylcytidine-2′-*O*-methyl-3′-*O*-(β-cyanoethyl-*N*,*N*-diisopropyl) phosphoramidite, 6-[4′-(hydroxymethyl)-4,5′,8-trimethylpsoralen] hexyl-1-*O*-(β-cyanoethyl-*N*,*N*-diisopropyl) phosphoramidite, and 8-hydroxy-5′-dimethoxytrityl-N^6-benzoyl-deoxyadenosine-3′-[(2-cyanoethyl)(*N*,*N*-diisopropyl)] phosphoramidite were purchased from Glen Research, Inc., Sterling, VA. The modified nucleosides 5′-*O*-(4,4′-dimethoxytrityl)-5-methyluridine-2′-*O*-(2-aminoethyl)-3′-*O*-(β-cyanoethyl-N,*N*-diisopropyl) phosphoramidite and N^4-(*N*-methylpyrrolidineamidine)-5′-*O*-(4,4′-dimethoxytrityl)-5-methylcytidine-2′-*O*-(2-aminoethyl)-3′-*O*-(β-cyanoethyl-*N*,*N*-diisopropyl) phosphoramidite were synthesized as described (*25*). All the reagents used for oligonucleotide synthesis were standard and were obtained from Chemgenes, Ashland, MA. [[γ]-^{32}P]ATP was purchased from Amersham Inc., and T_4 polynucleotide kinase was purchased from United States Biochemical Corp. Thin-layer chromatography (TLC) was performed on silica gel $60F_{254}$ plates (0.2 mm), and flash chromatography was carried out using EM Science Kieselgel 60 (230−400 mesh). Proton NMR spectra were recorded on a JEOL 400 MHz spectrometer with tetramethylsilane as reference for chemical shift. Electrophoresis was carried out in 12% polyacrylamide gels with or without 7 M urea. The TAE running buffer contained 40 mM Tris, 10 mM $MgAc_2$, and 5 mM NaAc buffered at pH 7.0. Reversed phase HPLC was carried out using a Symmetry 300 C_{18} column from Waters on a Shimadzu HPLC system (LC-10ADvp) with a duel wavelength detector (SPD-10AVvp) and an autoinjector (SIL-10AVvp).

Synthesis of Pseudoisocytidine Phosphoramidite. The synthesis of 2-[[(dimethylamino)methylene]amino]-5-[2-*O*-methyl-5-*O*-(dimethoxytrityl)-β-D-ribofuranosyl]-4(1H)-pyrimidinone-N^2-[(dimethylamino)methylene]-2′-*O*-methyl-5′-*O*-(dimethoxytrityl)-pseudoisocytidine-3′-*O*-(β-cyanoethyl-*N*,*N*-diisopropyl) phosphoramidite was done using the route reported previously (*19*). This involved conversion of pseudouridine to 1,3-dimethyl-3′-5′-*O*-(tetraisopropyldisiloxanyl)pseudouridine followed by methylation of the 2′-hydroxy group. Then deprotection of the silyl group,

reprotection of 5′-hydroxy group with dimethoxytrityl, guanidinylation, and finally the protection of the amino group by (*N*,*N*-dimethylamino)methylene gave 2-[[(dimethylamino)methylene]amino]-5-[2-*O*-methyl-5-*O*-(dimethoxytrityl)-β-D-ribofuranosyl]-4(1H)-pyrimidinone-N^2-[(dimethylamino)-methylene]-2′-*O*-methyl-5′-*O*-(dimethoxytrityl)pseudoisocytidine. Phosphitylation of the 3′-hydroxy group gave the expected pseudoisocytidine phosphoramidite, which was confirmed by NMR and MS analysis.

Oligonucleotide Syntheses. The oligonucleotides were synthesized on CPG supports using an Expedite model 8909 DNA/RNA synthesizer. All protected nucleoside phosphoramides were dissolved in anhydrous acetonitrile at a concentration of 0.05 M. The nucleoside pseudoisocytidine phosphoramidite solution was stored for 2 h over molecular sieves prior to use. Standard coupling times were employed for general nucleosides, except for pseudoisocytidine phosphoramidite and for the psoralen phosphoramidites, for which 360 and 600 s, respectively, were used. The synthesizer was programed to carry out a capping step, an oxidation step, and then another capping step after each coupling step and finally to remove the last 5′-terminal dimethoxytrityl group from the protected oligomer. The psoralen-derivatized oligomers were prepared on the controlled pore glass support using 2-[4′-(hydroxymethyl)-4,5′,8-trimethylpsoralen]hexyl-1-*O*-[(2-cyanoethyl)-(*N*,*N*-diisopropyl)] phosphoramidite in the final coupling reaction.

Deprotection and Purification of Oligonucleotides. The non-psoralen oligonucleotides were deprotected by treatment with a solution of 28−30% ammonium hydroxide at 55 °C for 5 h. Oligonucleotides containing 8-oxoadenine and pseudoisocytidine were deprotected by treating the support-bound oligomer with a solution of ethylenediamine in 95% ethanol (1:1 v/v) at room temperature for 16 h. Psoralen linked oligonucleotides were incubated in a 1:1 mixture of 28% ammonium hydroxide and 40% aqueous methylamine solution, at room temperature for 90 min. The deprotected oligomers were taken up in distilled water and purified by analytical and semipreparative anion exchange (IE) HPLC using a DIONEX DNAPac column on a Shimadzu HPLC system (LC-10ADvp) with a dual wavelength detector (SPD-10ADvp) and an autoinjector (SIL-10AVvp). The column was eluted using a linear gradient of 0−50% acetonitrile in 100 mM Tris-HCl buffer (pH 7.8) at a flow rate of 1.5 mL/min and monitored at 254 and 315 nm. The oligomers were desalted on a SEP PAK C_{18} cartridge following standard procedures. The purified oligomers migrated as single bands on 12% polyacrylamide gels and were characterized by matrix-assisted laser desorption−ionization time-of-flight (MALDI TOF) mass spectrometry.

Thermal Stability Measurements. The constituent strands of the target duplexes (1 μM) were dissolved in buffer containing 100 mM NaCl, 2 mM $MgCl_2$, and 10 mM Na-cacodylate, pH 7.0. The solutions were heated at 80 °C for 3 min and allowed to come to room temperature. The TFOs (1 μM) were added to the duplex solution and incubated at room temperature overnight. The thermal denaturation experiments were carried out using a Cary 3E UV−vis spectrophotometer fitted with a thermostated sample holder and temperature controller. Triplexes were heated from 10 to 85 °C at a rate of 0.4 °C/min, and the absorbance at 260 nm was recorded as a function of the temperature. All analyses were performed at least two times with an error of no more than 0.5 °C.

TFO Association Analysis by Absorbance Decay. The TFO + duplex → triplex transition is accompanied by a decrease in UV absorbance. This decay curve has been used to estimate the association rates of a TFO with the target duplex (*29*). For our experiments, the duplex strand was formed in kinetics buffer I (1 mM $MgCl_2$, 10 mM sodium cacodylate (pH 7.2), 150 mM KCl) to give a final concentration of 1 μM. 1 mL of the duplex stock solution was monitored by UV in a cuvette at 25 °C and gave a horizontal line as a function of time. The analyses were done at 25 °C (using a Peltier temperature controller). An aliquot of the TFO stock solution in kinetics buffer I was added with vigorous mixing to 1 mL of duplex stock solution. The mixing process took less than 10 s. The experiments were run on a Cary dual beam spectrophotometer. The decay curves were fit using second order kinetics with the software supplied with the instrument. Rate constants were reported as an average of three or more experiments.

Band Shift Analysis of Triplex Formation. The pyrimidine strand of the duplex was labeled with ^{32}P, the duplex formed, and then the triplex formed by incubation of the duplex (∼1 nM) and the third strand (2 μM) overnight in triplex formation buffer. The samples were then electrophoresed on 12% neutral polyacrylamide gels, in 10 mM Tris acetate (pH 7.0), 5 mM $MgCl_2$.

Psoralen Integrity Assay. After triplex formation on a ^{32}P labeled duplex, the samples were exposed to UVA (365 nM) for 10 min and then denatured by heating in loading buffer (containing 90% formamide) and then electrophoresed in a 12% denaturing polyacrylamide gel in 10 mM Tris borate, pH 8.0, 7 M urea.

Cross-linking of the Triplex Target in the Human β-Globin Gene in Cultured Cells. Human erythroleukemia K562 cells were suspended in a 100 μL solution with TFO-22 at 4 μM and then electroporated (Amaxa). The cells were suspended in medium and incubated for 3 h at room temperature. They were then exposed to UVA (365 nM) for 3 min in a Rayonet chamber at 1.8 J/cm^2. Genomic DNA was then extracted from the cells, purified, and then digested with *EcoRI* restriction enzyme (see ref *7* for details on the extraction and purification procedure). The digested samples were denatured by heating in 90% formamide and then electrophoresed in a neutral 1.5% agarose gel. The gel was blotted onto a nylon filter which was hybridized with a ^{32}P labeled probe against the human β-globin gene in a 5 kb restriction fragment.

RESULTS

*The β-Globin IVS2 Target Sequence.*The human β-globin gene consists of three exons and two introns. Inside the second intron is a 21 base polypurine:polypyrimidine element terminated by a 5′ TA step, which is a favored site for psoralen cross-linking (Figure 1). The triplex target sequence contains four adjacent cytosines. We began our studies by characterizing a series of pyrimidine and purine TFOs, containing adjacent cytosines or 5 methylcytosines and with different base, sugar, and backbone modifications, all shown to enhance triplex stability. The base modification was 5-(1-propynyl)-2′-deoxyuridine (pdU) (*30*). The sugar modifica-

Table 1: Sequence and Composition of TFOs Containing Adjacent C or 5MeC (Pyrimidine Motif) or G (Purine Motif) Residues[a]

TFO	base	sugar
TCTTTTCTTCCCCTTTCTTTT	5MeC	deoxy
AAAAGAAAGGGGAAGAAAAGA	A, G	deoxy
UCUUUUCUUCCCCUUUCUUUU	5MeC/pdU	deoxy
U*CU*U*U*U*CTTCCCCTTTCTTTU*	5MeC/T/U*	2′-OGE*, 2′-OMe
TCTTTTCTTCCCCTTTCTTTU∧	5MeC	2′-OMOE, 3′-OMOE∧
$TCTTTTCTTC_{AE}C_{AE}C_{AE}C_{AE}TTTCTTTT$	5MeC	2′-AE, 2′-OMe
$TCTTTTCTTCC_{AE}C_{AE}CTTTCTTTT$	5MeC	2′-AE, 2′-OMe
TGTTTTGTTGGGGTTTGTTTT	G, T	deoxy
$T_LCT_LTT_LTC_LTTLCCLCC_LTT_LTC_LTT_LT$	C, T	LNA (alt)
$(UCUUUUCUUCCCCUUUCUUU)_{MA}$ U	5MC/5MeU	2′-OMA
$TCTTTTCTTCCCCTTTCTTTT_{-(MORPH)}$	C, T	morpholino
A+G+A+A+A+G+G+G+G+A+A+G+A+A+A+A+G+A+	A, G	DEED

[a] AE, 2′-aminoethoxy; pdU, 5-(1-propynyl)-2′-deoxyuridine; OGE, 2′-*O*-(2-guanidoethyl)-5 methyl-U); OMOE, methoxyethyl; LNA, 2′-*O*,4′-*C*-methylene linked locked nucleic acid; OMA, 2′-*O*-(*N*-(methyl)acetamido)-5-methyl; MORPH, morpholino; DEED, diethylethylenediamine. The TFO containing the OGE derivative has the OGE sugar modification linked to 5 methyl-U.

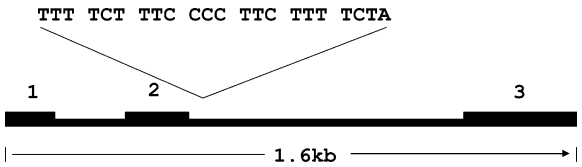

FIGURE 1: Organization of the human β-globin gene and the sequence of the triplex target in Intron 2.

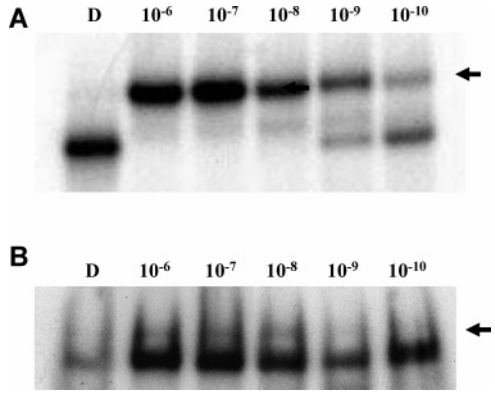

FIGURE 2: Band shift analysis of the deoxyribose TFO with adjacent 5-methylcytosines in the cytosine run: (A) pH 5.6; (B) pH 7.2. The arrow marks the position of the triplex. The lane marked D had only the duplex. The concentration of the TFO in each incubation is indicated at the top of the lane. These results were typical of the binding assays performed with the TFOs in Table 1.

tions were 2′-guanidoethyl (2′-OGE) (*31*), 2′-*O*,4′-*C*-methylene ribose (BNA/LNA) (*32*, *33*), 2′-*O*-(2-methoxyethyl) (2′-OME) (*34*), 2′-*O*-(*N*-(methyl)acetamido) (*35*), morpholino (*36*), 2′-*O*-methyl (2′-OMe), and 2′-aminoethoxy (2′-AE) (*25*). The backbone modification was the nonbridging phosphate derivative diethylethylenediamine (DEED) (*37*). Target binding by the TFOs shown in Table 1 was analyzed in a band shift assay at pH 5.6 and 7.2**.** While a number of the TFOs were able to form stable triplexes at pH 5.6 (a representative example is shown in Figure 2), they either showed weak binding (the DEED TFO, $K_d = 10^{-6}$) or no binding (all other TFOs) at pH 7.2. Of particular interest were the TFOs containing 2′ AE residues in the cytosine patch. The AE moiety is positively charged at neutral pH and has been shown to stabilize triplexes (*25*). The band shift assays with all the oligonucleotides, including the AE TFOs, indicated that the inhibitory effect of the cytosine run overcame substitutions that otherwise stabilize triplexes at neutral pH.

Duplex 1
5′-ATGTTTTCTTT CCCC TTCTTTTCTATGG
3′-TACAAAAGAAA GGGG AAGAAAAGATACC

Duplex 2
5′-ATGTTTTCTTT TTTT TTCTTTTCTATGG
3′-TACAAAAGAAA AAAA AAGAAAAGATACC

Duplex 3
5′-ATGTTTTCTTT CTCT TTCTTTTCTATGG
3′-TACAAAAGAAA GAGA AAGAAAAGATACC

Duplex 4
5′-ATGTTTTCTTT CTTC TTCTTTTCTATGG
3′-TACAAAAGAAA GAAG AAGAAAAGATACC

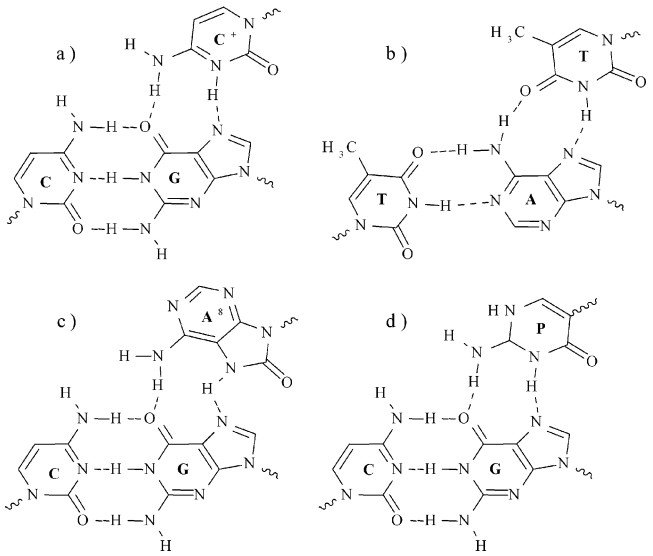

FIGURE 3: (A) Sequence of the human β-globin triplex target, and variants. The four clustered G:C pairs are separated from the remainder of the sequence, and the psoralen cross-link site is indicated in larger font. In duplex 2 the adjacent G:C pairs were replaced with A:T. In duplex 3 G:C and A:T pairs were alternated, while in duplex 4 the G:C flanked adjacent A:T pairs. (B) Structure of (a) C^+·G:C, (b) T·A:T, (c) 8-oxo-A (A^8)·G:C, and (d) 2′-*O*-methylpseudoisocytidine (P)·G:C triplets.

All of the pyrimidine TFOs contained cytosine or 5MeC, both isolated and adjacent. The failure of these constructions prompted us to consider the effect of substitutions of cytosine replacements within the cytosine patch. C^+·G:C or 5-MeC^+·G:C triplets are stabilized by hydrogen bonding, and also the positive charge, which appears to make a major contribution (*12*). However, cytosine replacements, such as 8-oxoadenine (A^8) or 2′-*O*-methylpseudoisocytidine (P) (Figure 3A), used in the following experiments, lack the positive charge.

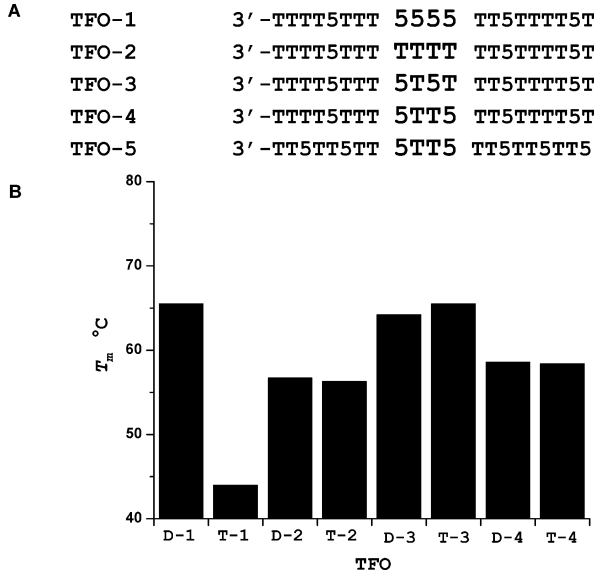

FIGURE 4: (A) Sequence of TFOs designed to bind duplexes 1−4. TFO-5 is a scrambled control. 5 = 5-methylcytosine; all sugars were 2′-OMe ribose. (B) Thermal stability of duplexes 1−4 and the triplexes formed by TFOs-1−4. D = duplex; T = triplex.

To assess the consequences for triplex stability of the loss of the protonated cytosine charge, we synthesized duplex targets for binding studies in which all (duplex 2) or two of the four cytosines (duplexes 3 and 4) were replaced with T (Figure 3B). These targets provided the opportunity to examine the stability of complexes in which the T·A:T triplets would provide a reference for triplets formed by the uncharged cytosine replacements.

We prepared triplexes with the duplexes and the corresponding TFOs shown in Figure 4A. The third strands contained 5-MeC as indicated, and all sugars were 2′-OMe ribose. TFO-5 was prepared as a scrambled sequence control. Thermal stability analysis demonstrated that the T_m value of the duplex containing the β-globin target sequence was 65.5 °C, while the sequences of the other duplex targets were similar (duplex 3, 64.2 °C) or reduced, reflecting the alterations in sequence context and the replacement of C with T (duplex 2, 56.7 °C; duplex 4, 58.4 °C) (Figure 4B). In previous work we, and others, found that triplexes, with isolated cytosines, formed by TFOs containing 2′-OMe ribose at all positions had T_m values that were similar to that of the underlying duplex at neutral pH (*28*, *38*). This was observed with the triplexes formed on the variant duplexes 2, 3, and 4. However, the destabilizing effect of the adjacent (5-Me) cytosines was readily apparent in the analysis of the triplex formed by TFO-1 on duplex 1, as the T_m value was 21.5 °C lower than that of the duplex. The scrambled control TFO-5 failed to make a stable triplex.

TFOs Containing A[8]. Third strands were synthesized with A^8 variously used as a cytosine replacement (Figure 5A). These oligonucleotides were designed to examine the effect of adjacent A^8 residues (TFO-7, -8, -9) as well as in alternation with 5-MeC. A TFO in which all cytosine positions were replaced by A^8 was also prepared (TFO-11). This TFO was unable to form a triplex. However, the other oligonucleotides in this group formed triplexes that were more stable than that formed by TFO-1, as illustrated for TFO-9 in the first derivative plot in Figure 5B. The most stable triplexes were formed by TFOs-7, -9, -10, with T_m

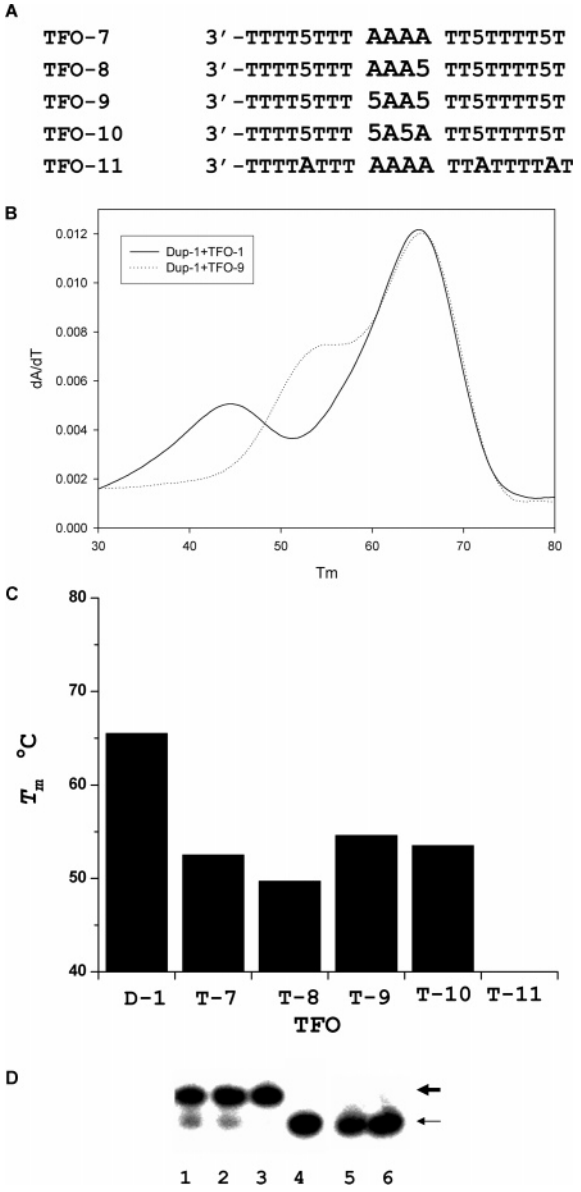

FIGURE 5: Characterization of TFOs with A^8. (A) Sequence of TFOs with different arrangements of A^8 in the adjacent G:C patch. (B) First derivative curve of thermal stability analysis of the triplexes formed by duplex 1 and TFO-1, and duplex 1 and TFO-9. (C) T_m values for the triplexes formed by TFOs-7−10. For reference the value for duplex 1 is also shown. (D) Band shift analysis of triplexes formed by TFOs containing A^8: lanes 1−3, triplexes formed by TFOs-10, -9, and -7, respectively; lane 4, duplex 1 + TFO-1; lane 5, duplex 1 + TFO-5 (scrambled control); lane 6, duplex 1. The light arrow marks the duplex, and the heavy arrow, the triplex.

values 8−10 degrees higher than that with TFO1 (Figure 5C). Band shift analysis confirmed the formation of stable triplexes by TFOs-7, -9, and -10 but not by TFO-1 or the scrambled control TFO-5 (Figure 5D).

Although TFOs-7−10 were an improvement relative to TFO-1, their triplexes were not as stable as the duplex target. This would be expected given the absence of positive charge on A^8. However, comparison with the results with the cognate triplexes shown in Figure 4 indicated that triplexes with A^8·A:T triplets were less stable than triplexes with T·A:T triplets at the corresponding positions. Thus, the absence of the positive charge did not completely explain the relatively low T_m values.

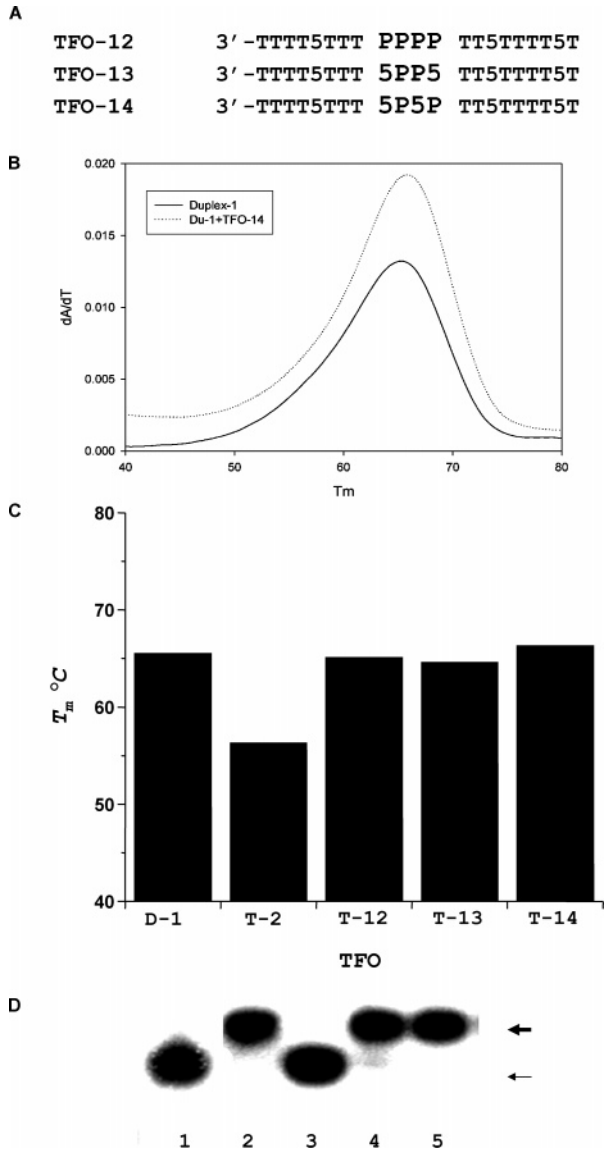

FIGURE 6: Characterization of triplexes formed by TFOs with P substitution. (A) Sequence of TFOs-12−14. (B) First derivative of thermal stability analysis of duplex 1 and the triplex formed by duplex 1 and TFO-14. (C) Thermal stability of triplexes formed by duplex 1 and TFOs-12−14. For comparison the T_m value for duplex 1 and the triplex on the variant duplex with four adjacent A:T pairs (compare with T-12) are shown. (D) Band shift analysis of triplexes formed by TFOs-12−14: lane 1, duplex 1 + TFO-1; lane 2, duplex 1 + TFO-12; lane 3, duplex 1 + TFO-5; lane 4, duplex 1 + TFO-13; lane 5, duplex 1 + TFO-14. The light arrow marks the duplex, and the heavy arrow, the triplex.

TFOs Containing P. TFOs-12−14 were synthesized. These replaced cytosine with pseudoisocytidine in the same pattern as the TFOs with A[8] (Figure 6A). Thermal analysis of the triplex formed by TFO-14 (with the alternation of P and 5-MeC) yielded a T_m slightly higher than that of the duplex (66.3 vs 65.5 °C (Figure 6B)). Indeed the T_m values for the triplexes formed by TFOs-12−14 were similar to the value for the duplex target (Figure 6C). Band shift analysis confirmed triplex formation by the three TFOs (Figure 6D). These results were encouraging, as they suggested that P could effectively replace cytosine in runs of adjacent cytosines, producing TFOs that could form quite stable triplexes at neutral pH.

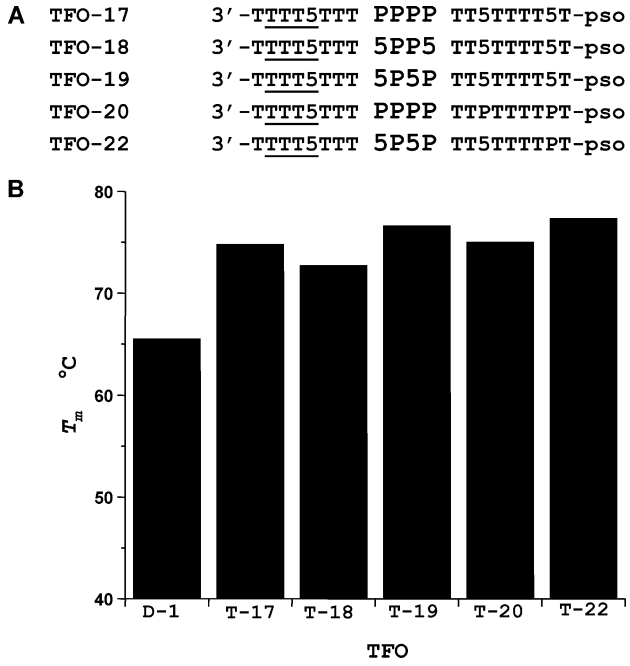

FIGURE 7: Characterization of TFOs containing P substitutions and a patch of AE residues. (A) TFO sequences; AE residues are underlined; P = pseudoisocytidine. (B) T_m values. (C) Psoralen activity analysis on denaturing acrylamide gel: lane 1, ^{32}P labeled pyrimidine strand of the duplex; lanes 2−6, duplex 1 + TFOs-17−20 and -22; lane 7, duplex 1 + TFO 17, no UVA.

TFOs with P and AE Substitutions. In our earlier work with TFOs designed to target a site in the *HPRT* gene, we found that a patch of three our four AE residues (all others being 2′-OMe) made an essential contribution to bioactivity (*27*, *28*). Accordingly, we prepared TFOs containing a patch of four AE residues at the 3′ end and different patterns of P substitution (Figure 7A). The introduction of AE residues increased the T_m values for all the TFOs (Figure 7B). The TFOs with different patterns of the P substitution showed marked increases. TFO-19, for example, with the alternation of 5-MeC and P, had a T_m value of 76.6 °C, approximately 12 °C higher than that for the underlying duplex. In a separate analysis we found that the psoralen does not make a measurable contribution to the T_m value (not shown). Triplex formation was confirmed by band shift analysis (not shown). Complete conversion of the labeled duplex to triplex was observed with TFOs-17, -18, and -19. It was noteworthy that the pattern of P substitution in the cytosine run did not appear to be critical, since the oligonucleotide with four contiguous P residues (TFO-17) was as effective in both assays as TFOs-18 and -19, with nonadjacent P substitutions.

The P replacement for cytosine is noncharged, and we were curious as to the consequences of replacement of isolated cytosines in the TFOs. Two additional oligonucleotides were synthesized. One was based on TFO-19 and had one additional P residue near the 5′ end (TFO-22). In the second, all but one cytosine were replaced with the P substitution (TFO-20). Both these TFOs formed quite stable triplexes, as indicated by the T_m values and the band shift analysis (Figure 5 B and C), essentially equivalent to the other TFOs in this group.

The TFOs in the AE-P group were linked to psoralen. Psoralen is labile to alkali, and it was important to ensure that it was still active after deprotection (we used a different

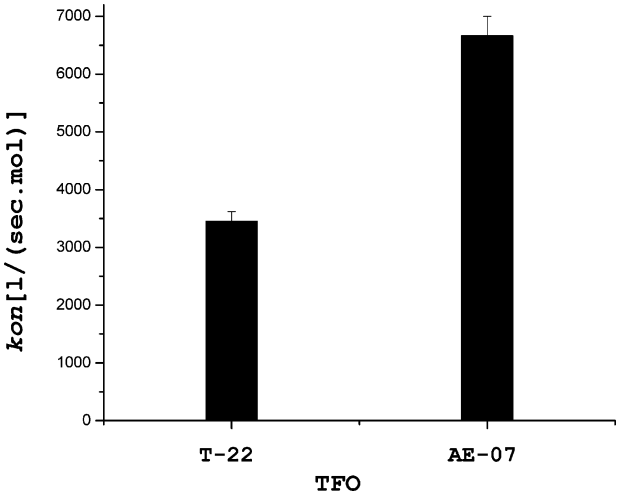

FIGURE 8: Relative association rate of TFO 22. Also shown is the value for AE−07, which contains a patch of 4 AE residues and was designed for the *HPRT* target.

procedure than in previous work) and purification. We prepared triplexes on radioactively labeled duplex and then exposed the preparations to long wavelength ultraviolet light to photoactivate the psoralen. The samples were then electrophoresed on polyacrylamide gels in the presence of 7 M urea. The urea denatures the triplex and thus resolves three strand complexes linked via psoralen, while non-cross-linked molecules migrate with the unconjugated, denatured duplex strands. This assay verified the integrity of the psoralen, which was essential for the analysis of the biological activity of the TFOs (data not shown).

Association Rate of the AE-P TFOS. Recently we compared the biochemical and biophysical parameters of TFOs containing AE substitutions with the biological activity data (*27*). We were attempting to find a biophysical measure of triplex formation that correlated with the biological activity profile. We concluded that the k_{ON} was a much better predictor of bioactivity than the T_m value. Following this observation, we measured the relative association rate for TFO-22, which formed the triplex with the highest T_m value. The results indicated that this TFO had a k_{ON} value that was within a factor of 2−3 of the value of the bioactive TFO developed for the hamster *HPRT* target (TFO-AE-07, Figure 8).

Bioactivity of the AE-P TFOs. These results suggested that the principles regarding modification format, derived from our work with the *HPRT* target TFOs, could be extended to other targets. However, it was essential to assay the TFOs in a procedure that would report target binding in living cells. In a previous publication we showed that a psoralen linked TFO could introduce a cross-link into the *HPRT* target at sufficiently high levels to allow detection of the cross-link as a biochemical entity. We took advantage of the well-known denaturation resistance assay of cross-linked restriction fragments (*39*), in which denatured, non-cross-linked DNA fails to reanneal upon entry into a neutral environment, while cross-linked strands snap back to the duplex form. The denatured and snap-back duplex fragments have different electrophoretic mobilities in agarose gels, and the amount of snap-back target DNA can be used as a measure of targeted cross-linking (*7*). TFO-22 was introduced into erythroleukemia K562 cells by electroporation. After 3 h the cells were exposed to UVA to photoactivate the psoralen. DNA was extracted from the cells and then digested with *EcoRI*, generating a 5 kb fragment containing the triplex target site. The DNA digests were denatured and electrophoresed in a neutral agarose gel. The gel was blotted and then hybridized with a β-globin gene probe. As expected, the band in the nondenatured sample migrated more slowly than that in the denatured control sample. While there was no detectable band at the nondenatured position in the DNA isolated from untreated cells, there was a readily detected band in the snap-back position in DNA from cells treated with TFO-22. Results from two independent experiments are shown in Figure 9A. Analysis of the band intensity by densitometry indicated that about 10% of the target DNA was in the cross-linked band. We have shown previously that this analysis under-reports the actual extent of cross-linking by about 2-fold (*40*). In a parallel analysis the digested DNA was examined by hybridization with a probe against the dihydrofolate reductase gene. There was no denaturation resistant band in this pattern (Figure 9B). These results demonstrated that TFO-22 was capable of finding and binding the β-globin IVS2 target sequence in living human cultured cells. Furthermore, the lack of cross-linking in the DHFR gene argued for targeting specificity, at least at the level of the gene.

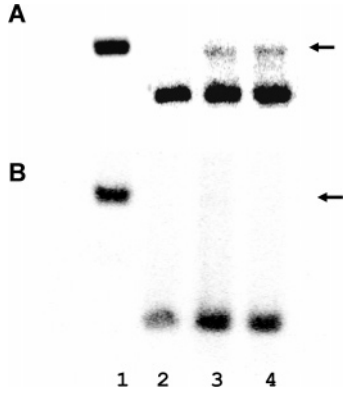

FIGURE 9: Denaturation resistance analysis of genomic DNA isolated from K562 cells treated with TFO-22/UVA. The DNA was isolated and digested with EcoRI, which generates a 5.6 kb fragment containing the β-globin gene. Samples were then denatured and electrophoresed on a neutral agarose gel, followed by Southern blotting. (A) Pattern of hybridization with a probe against the β-globin gene. (B) Pattern of hybridization with a probe against the DHFR gene. The arrows show the position of the denaturation resistant fragment: lane 1, nondenatured DNA from untreated cells; lane 2, denatured DNA from untreated cells; lanes 3 and 4, denatured DNA from independent treatments.

DISCUSSION

There are a number of challenges to the development of TFOs with biological activity in living mammalian cells. Several are fundamental to the chemistry and biophysical properties of the oligonucleotides and their sequence targets. These include the charge repulsion between the third strand and the duplex, and the requisite conformation restrictions on the third strand in a triplex. Sugar derivatives with the C3′-endo conformation—and the consequent preorganization of the third strand—provide some redress of the conformational issues (*9*). The inclusion of 2′AE residues relieves, at least in part, the charge repulsion problem (*25*, *26*). We have demonstrated bioactivity of TFOs containing these modifica-

tions against an uninterrupted polypurine:polypyrimidine element with nonadjacent cytosines (*27*, *28*).

The pyrimidine and purine motif TFOs listed in Table 1 incorporated a variety of sugar and backbone modifications in an effort to overcome the destabilizing influence of four adjacent cytosines or 5-methylcytosines. This was not a successful approach, as it did not produce triplexes that were stable at physiological pH. This failure prompted us to examine the utility of base analogues that could replace cytosine. We adopted as a working "rule of thumb" that the TFOs should form triplexes with T_m values similar, if not equal, to that for the underlying duplex at neutral pH. Although the TFOs with A^8 were an improvement on the TFOs in Table 1, they failed to satisfy this requirement. The A^8 TFOs formed triplexes that were less stable than those formed on the variant duplexes 2, 3, and 4, in which thymidines replaced cytosines so as to avoid adjacent cytosines. These variant targets were designed to measure the stability of triplexes without the contribution of the positive charge of a protonated cytosine. The comparison with these triplexes and those formed by the A^8 suggests that the relative instability of the A^8 triplexes was due to more than the simple loss of the positive charge. It is likely that this can be explained by structural distortion resulting from the presence of the purine analogue in the midst of a pyrimidine motif third strand.

Triplexes formed by TFOs with the P analogue were clearly more stable than those with A^8. We were able to prepare triplexes with TFOs containing various combinations of P, all in the context of 2′-OMe-ribose sugar substitutions, that had thermal stability similar to or slightly greater than that of the underlying duplex. It was noteworthy that the T_m values of these triplexes were higher than those of the corresponding variant triplexes in which T was substituted for C so as to avoid adjacent cytosines. The greatest T_m value differentials were seen with the triplexes in which there were four adjacent P residues (TFO-12, 65.1 °C) or four adjacent thymidines (TFO-2, 56.3 °C) as compared to triplexes in which the T and C, or T and P, residues were alternated: TFO-14 (66.3 °C) versus TFO-3 (65.5 °C). We had expected that the triplexes with P would have similar stability as those with a corresponding T. The greater stability of the triplexes with the adjacent P substitutions may be due to stabilizing interactions contributed by the P residues that are not possible from thymidines. It may also be that the Hoogsteen hydrogen bonds formed by the P analogue are more stable than those formed by thymidine.

Targeting a Nonreporter Gene. Our previous work with TFOs designed to target genomic sequences took advantage of the mutation reporter feature of the *HPRT* gene. The *HPRT* target site also had a restriction recognition sequence that enabled targeted cross-linking, and mutagenesis, to be measured by restriction enzyme resistance (*7*). The β-globin gene IVS2 triplex target sequence presented the challenge of measuring TFO targeting efficiency in the absence of a reporter gene function or the presence of a conveniently placed restriction enzyme recognition sequence. Since these conditions will describe most genomic targets of interest, it was important to demonstrate the feasibility of constructing pso-TFOs with sufficient bioactivity to enable detection by virtue of the targeted cross-link. Restriction fragment denaturation resistance provides a well-established method for cross-link detection (*39*). The data in Figure 9A demonstrate that a TFO containing AE and P substitutions is active as measured in this assay. It should be noted that the assay is relatively insensitive (*7*). Nicks anywhere in a cross-linked strand, introduced during extraction, purification, and digestion of the genomic DNA, will result in the loss of material in the snap-back band. In addition, the cross-linking can interfere with blotting and hybridization. Consequently, the intensity of the cross-linked band is an underestimate of the actual extent of cross-linking. We estimate that the total extent of cross-linking of the β-globin gene IVS2 target was at least 15%. Although there is room for improvement, these results suggest that the AE modification format identified in our earlier work (*28*) can be extended to other genomic targets. Furthermore, it appears that the P substitution is an effective solution to the problem of adjacent cytosines in pyrimidine motif triplexes. The efficacy of the P substitution suggests that other base analogues whose biochemical characteristics appear promising will be effective in biological assays. It will be of considerable interest to test not only additional cytosine replacements (*20*, *22*, *23*) but also analogues designed to overcome current restrictions on triplex sequence options (*41*, *42*).

β-Globin Expression in K562 Cells. K562 cells do not transcribe the β-globin gene. The cells express specific repressor proteins that bind to elements upstream of the promoter (*43*). Suppression of expression of one of these proteins results in transcription of the β-globin gene (*44*). In previous work we have shown that access to the *HPRT* triplex target is enhanced in S phase cells (*7*). Transcriptional activity also improves target binding by TFOs (*8*). The results shown in Figure 9A imply that targets in nontranscribed genes may also be accessible to TFOs. Additional experiments will be required to determine the influence of cell cycle status and transcriptional activity on TFO activity against the β-globin target.

Recently, we have found that pso-TFOs can be used to target recombination of exogenous "donor" DNA at frequencies 3 orders of magnitude greater than when only donor DNA is introduced (manuscript in preparation). The experiments described in this report are an initial account of the development of a targeted gene conversion strategy for restoring function to mutant β-globin genes.

REFERENCES

1. Kang, E. M., and Tisdale, J. F. (2004) The leukemogenic risk of integrating retroviral vectors in hematopoietic stem cell gene therapy applications, *Curr. Hematol. Rep. 3*, 274−281.
2. Felsenfeld, G., Davies, D. R., and Rich, A. (1957) Formation of a three stranded polynucleotide molecule, *J. Am. Chem. Soc. 79*, 2023−2024.
3. Goni, J. R., de, l. C. X., and Orozco, M. (2004) Triplex-forming oligonucleotide target sequences in the human genome, *Nucleic Acids Res. 32*, 354−360.
4. Fossella, J. A., Kim, Y. J., Shih, H., Richards, E. G., and Fresco, J. R. (1993) Relative specificities in binding of Watson−Crick base pairs by third strand residues in a DNA pyrimidine triplex motif, *Nucleic Acids Res. 21*, 4511−4515.
5. Brown, P. M., and Fox, K. R. (1998) DNA triple-helix formation on nucleosome-bound poly(dA)·poly(dT) tracts, *Biochem. J. 333* (Pt 2), 259−267.
6. Brown, P. M., and Fox, K. R. (1996) Nucleosome core particles inhibit DNA triple helix formation, *Biochem. J. 319* (Pt 2), 607−611.
7. Majumdar, A., Puri, N., Cuenoud, B., Natt, F., Martin, P., Khorlin, A., Dyatkina, N., George, A. J., Miller, P. S., and Seidman, M.

M. (2003) Cell Cycle Modulation of Gene Targeting by a Triple Helix-forming Oligonucleotide, *J. Biol. Chem. 278*, 11072−11077.
8. Macris, M. A., and Glazer, P. M. (2002) Transcription dependence of chromosomal gene targeting by triplex-forming oligonucleotides, *J. Biol. Chem. 278*, 3357−3362.
9. Asensio, J. L., Carr, R., Brown, T., and Lane, A. N. (1999) Conformational and thermodynamic properties of parallel intramolecular triple helixes containing a DNA, RNA, or 2′-OMeDNA third strand, *J. Am. Chem. Soc. 121*, 11063−11070.
10. Lee, J. S., Woodsworth, M. L., Latimer, L. J., and Morgan, A. R. (1984) Poly(pyrimidine). poly(purine) synthetic DNAs containing 5- methylcytosine form stable triplexes at neutral pH, *Nucleic Acids Res. 12*, 6603−6614.
11. Leitner, D., Schroder, W., and Weisz, K. (2000) Influence of sequence-dependent cytosine protonation and methylation on DNA triplex stability, *Biochemistry 39*, 5886−5892.
12. Asensio, J. L., Lane, A. N., Dhesi, J., Bergqvist, S., and Brown, T. (1998) The contribution of cytosine protonation to the stability of parallel DNA triple helices, *J. Mol. Biol. 275*, 811−822.
13. Coman, D., and Russu, I. M. (2004) Site-resolved stabilization of a DNA triple helix by magnesium ions, *Nucleic Acids Res. 32*, 878−883.
14. Puri, N., Majumdar, A., Cuenoud, B., Natt, F., Martin, P., Boyd, A., Miller, P. S., and Seidman, M. M. (2001) Targeted gene knockout by 2′−O-aminoethyl modified triplex forming oligonucleotides, *J. Biol. Chem. 276*, 28991−28998.
15. Volker, J., and Klump, H. H. (1994) Electrostatic effects in DNA triple helices, *Biochemistry 33*, 13502−13508.
16. Sugimoto, N., Wu, P., Hara, H., and Kawamoto, Y. (2001) pH and cation effects on the properties of parallel pyrimidine motif DNA triplexes, *Biochemistry 40*, 9396−9405.
17. Miller, P. S., Bi, G., Kipp, S. A., Fok, V., and DeLong, R. K. (1996) Triplex formation by a psoralen-conjugated oligodeoxyribonucleotide containing the base analog 8-oxo-adenine, *Nucleic Acids Res. 24*, 730−736.
18. Ono, A., Ts'o, P. O., and Kan, L. (1991) Triple helix formation of oligonucleotides containing 2′−O-methylpseudoisocytidine in substitition for 2′-deoxycytidine, *J. Am. Chem. Soc. 113*, 4032−4033.
19. Ono, A., Ts'o, P. O., and Kan, L. (1992) Triplex formation of an oligonucleotide containing 2′−O-methylpseudoisocytidine with a DNA duplex at neutral pH, *J. Org. Chem. 57*, 3225−3230.
20. Hildebrandt, S., Blaser, A., Parel, S. P., and Leumann, C. J. (1997) 5-Substituted 2-aminopyridine C-nucleosides as protonated cytidine equivalents: increasing efficiency and selectivity in DNA triple helix formation, *J. Am. Chem. Soc. 119*, 5499−5511.
21. Bates, P. J., Laughton, C. A., Jenkins, T. C., Capaldi, D. C., Roselt, P. D., Reese, C. B., and Neidle, S. (1996) Efficient triple helix formation by oligodeoxyribonucleotides containing alpha- or beta-2-amino-5-(2-deoxy-D-ribofuranosyl) pyridine residues, *Nucleic Acids Res. 24*, 4176−4184.
22. Cassidy, S. A., Slickers, P., Trent, J. O., Capaldi, D. C., Roselt, P. D., Reese, C. B., Neidle, S., and Fox, K. R. (1997) Recognition of GC base pairs by triplex forming oligonucleotides containing nucleosides derived from 2-aminopyridine, *Nucleic Acids Res. 25*, 4891−4898.
23. Xiang, G., Bogacki, R., and McLaughlin, L. W. (1996) Use of a pyrimidine nucleoside that functions as a bidentate hydrogen bond donor for the recognition of isolated or contiguous G−C base pairs by oligonucleotide-directed triplex formation, *Nucleic Acids Res. 24*, 1963−1970.
24. Mayer, A., Haberli, A., and Leumann, C. J. (2005) Synthesis and triplex forming properties of pyrrolidino pseudoisocytidine containing oligodeoxynucleotides, *Org. Biomol. Chem 3*, 1653−1658.
25. Cuenoud, B., Casset, F., Husken, D., Natt, F., Wolf, R. M., Altmann, K. H., Martin, P., and Moser, H. E. (1998) Dual recognition of double stranded DNA by 2′-aminoethoxy-modified oligonucleotides, *Angew. Chem., Intl. Ed. 37*, 1288−1291.
26. Blommers, M. J., Natt, F., Jahnke, W., and Cuenoud, B. (1998) Dual recognition of double-stranded DNA by 2′-aminoethoxy-modified oligonucleotides: the solution structure of an intramolecular triplex obtained by NMR spectroscopy, *Biochemistry 37*, 17714−17725.
27. Puri, N., Majumdar, A., Cuenoud, B., Miller, P. S., and Seidman, M. M. (2004) Importance of Clustered 2′−O−(2-Aminoethyl) Residues for the Gene Targeting Activity of Triple Helix-Forming Oligonucleotides, *Biochemistry 43*, 1343−1351.
28. Puri, N., Majumdar, A., Cuenoud, B., Natt, F., Martin, P., Boyd, A., Miller, P. S., and Seidman, M. M. (2002) Minimum Number of 2′-O-(2-Aminoethyl) Residues Required for Gene Knockout Activity by Triple Helix Forming Oligonucleotides, *Biochemistry 41*, 7716−7724.
29. Arya, D. P., Coffee, R. L., Jr., Willis, B., and Abramovitch, A. I. (2001) Aminoglycoside-nucleic acid interactions: remarkable stabilization of DNA and RNA triple helices by neomycin, *J. Am. Chem* Soc. *123*, 5385−5395.
30. Lacroix, L., Lacoste, J., Reddoch, J. F., Mergny, J. L., Levy, D. D., Seidman, M. M., Matteucci, M. D., and Glazer, P. M. (1999) Triplex formation by oligonucleotides containing 5-(1-propynyl)-2′-deoxyuridine: decreased magnesium dependence and improved intracellular gene targeting, *Biochemistry 38*, 1893−1901.
31. Prakash, T. P., Puschl, A., Lesnik, E., Mohan, V., Tereshko, V., Egli, M., and Manoharan, M. (2004) 2′-O-[2-(guanidinium)ethyl]-modified oligonucleotides: stabilizing effect on duplex and triplex structures, *Org. Lett. 6*, 1971−1974.
32. Obika, S., Uneda, T., Sugimoto, T., Nanbu, D., Minami, T., Doi, T., and Imanishi, T. (2001) 2′-O,4′-C-Methylene bridged nucleic acid (2′, 4′-BNA): synthesis and triplex-forming properties, *Bioorg. Med. Chem 9*, 1001−1011.
33. Jepsen, J. S., Sorensen, M. D., and Wengel, J. (2004) Locked nucleic acid: a potent nucleic acid analog in therapeutics and biotechnology, *Oligonucleotides 14*, 130−146.
34. Lind, K. E., Mohan, V., Manoharan, M., and Ferguson, D. M. (1998) Structural characteristics of 2′-O-(2-methoxyethyl)-modified nucleic acids from molecular dynamics simulations, *Nucleic Acids Res. 26*, 3694−3799.
35. Pattanayek, R., Sethaphong, L., Pan, C., Prhavc, M., Prakash, T. P., Manoharan, M., and Egli, M. (2004) Structural rationalization of a large difference in RNA affinity despite a small difference in chemistry between two 2′-O-modified nucleic acid analogues, *J. Am. Chem Soc. 126*, 15006−15007.
36. Summerton, J., and Weller, D. (1997) Morpholino antisense oligomers: design, preparation, and properties, *Antisense Nucleic Acid Drug Dev. 7*, 187−195.
37. Dagle, J. M., and Weeks, D. L. (1996) Positively charged oligonucleotides overcome potassium-mediated inhibition of triplex DNA formation, *Nucleic Acids Res. 24*, 2143−2149.
38. Shimizu, M., Konishi, A., Shimada, Y., Inoue, H., and Ohtsuka, E. (1992) Oligo(2′-O-methyl)ribonucleotides. Effective probes for duplex DNA, *FEBS Lett. 302*, 155−158.
39. Hartley, J. A., Souhami, R. L., and Berardini, M. D. (1993) Electrophoretic and chromatographic separation methods used to reveal interstrand crosslinking of nucleic acids, *J. Chromatogr. 618*, 277−288.
40. Majumdar, A., Puri, N., McCollum, N., Richards, S., Cuenoud, B., Miller, P., and Seidman, M. M. (2003) Gene Targeting by Triple Helix-Forming Oligonucleotides, *Ann. N. Y. Acad. Sci. 1002*, 141−153.
41. Rusling, D. A., Powers, V. E., Ranasinghe, R. T., Wang, Y., Osborne, S. D., Brown, T., and Fox, K. R. (2005) Four base recognition by triplex-forming oligonucleotides at physiological pH, *Nucleic Acids Res. 33*, 3025−3032.
42. Gowers, D. M., and Fox, K. R. (1999) Towards mixed sequence recognition by triple helix formation, *Nucleic Acids Res. 27*, 1569−1577.
43. Ebb, D., Tang, D. C., Drew, L., Chin, K., Berg, P. E., and Rodgers, G. P. (1998) Identification of upstream regulatory elements that repress expression of adult beta-like globin genes in a primitive erythroid environment, *Blood Cells, Mol. Dis. 24*, 356−369.
44. Zoueva, O. P., and Rodgers, G. P. (2004) Inhibition of beta protein 1 expression enhances beta-globin promoter activity and beta-globin mRNA levels in the human erythroleukemia (K562) cell line, *Exp. Hematol. 32*, 700−708.

BI0520986